Phase-Coherence Effects in Vortex Transport Entropy

G. Bridoux,* G. Nieva, and F. de la Cruz

Centro Atómico Bariloche and Instituto Balseiro, Comisión Nacional de Energía Atómica, Avenida E. Bustillo 9500, R84002AGP S. C. de Bariloche, Argentina

(Received 8 April 2008; published 10 September 2008)

Nernst and electrical resistivity measurements in superconducting $YBa_2Cu_3O_{7-\delta}$ and $Bi_2Sr_2CaCu_2O_{8+\delta}$ with and without columnar defects show a distinctive thermodynamics of the respective liquid vortex matter. At a field-dependent high temperature region in the H-T phase diagram, the Nernst signal is independent of structural defects in both materials. At lower temperatures, in $YBa_2Cu_3O_{7-\delta}$, defects contribute only to the vortex mobility, and the transport entropy is that of a system of vortex lines. The transition to lower temperatures in $Bi_2Sr_2CaCu_2O_{8+\delta}$ has a different origin; the maximum in the Nernst signal when decreasing temperature is not associated with transport properties but with the entropy behavior of pancake vortices in the presence of structural defects.

DOI: 10.1103/PhysRevLett.101.117002 PACS numbers: 74.25.Op, 74.25.Fy, 74.40.+k, 74.72.−h

The Nernst signal in superconductors is associated with the displacement of vortices induced by the presence of a temperature gradient ∇T perpendicular to the internal magnetic field $\mathbf{B}$. Its detection is made measuring the Josephson voltage induced by vortices crossing electrical contacts aligned in a direction perpendicular to both $\mathbf{B}$ and ∇T. For an ideal superconductor and straight vortex lines, if ∇T is in the $\hat{\mathbf{x}}$ direction $[(\nabla T)_x]$ and $\mathbf{B}$ in the $\hat{\mathbf{z}}$ direction, the Nernst electric field is proportional to $(\nabla T)_x$ [1]. Within this regime it was shown [1] that the thermal force per unit vortex length is $F_T(H) = S_\phi(H, T)(\nabla T)_x$. Here $S_\phi(H, T)$ is the transport entropy per unit vortex length. In this limit the impedance to vortex displacement is the flux flow vortex viscosity, associated with the flux flow electrical resistivity ρ_f. Thus, the Nernst signal is found [2]

$$e_N(H, T) = \frac{E_y}{(\nabla T)_x} = \frac{\rho_f S_\phi(H, T)}{\phi_0}, \tag{1}$$

where E_y is the Nernst electrical field and ϕ_0 the flux quantum. In the normal state, $e_N(T, H)$ is essentially zero [3], and, since $S_\phi(H, T) = 0$ at either $T = 0$ or H less than the lower critical field $H_{c1}(T)$, we see that e_N should show a maximum as a function of H or T.

In real materials, vortex pinning inhibits vortex displacements within an Ohmic regime [4]. Therefore, the maximum of $e_N(T, H)$ is usually determined by the field or temperature where pinning reduces vortex mobility to zero. In low T_c materials, this imposes strong limitations on the range of fields and temperatures where $e_N(T, H)$ can be used to determine $S_\phi(H, T)$. In high T_c superconductors, the short coherence length, strong material anisotropy and thermal energy are responsible for a transition from a solid to a liquid vortex state in a wide region of the H-T phase diagram. This phase diagram for a superconductor opened a renewed interest in the study of vortex physics: Solid-liquid phase transitions, vortex cutting and reconnection, low vortex dimensionality, vortex decoupling, and the contribution of thermal fluctuations play an important roll [5].

The pioneering work by Ri *et al.* [2] showed that the Nernst effect in films of $YBa_2Cu_3O_{7-\delta}$ (YBCO) and $Bi_2Sr_2CaCu_2O_{8+\delta}$ (BSCCO) responds, qualitatively, to the behavior expected from Ginzburg-Landau theory. Recent work by Ong and collaborators [3] triggered intensive experimental and theoretical activity.

Previous work on YBCO and BSCCO showed [6,7] that, using the dc flux transformer contact configuration in twinned YBCO crystals, the c axis vortex phase correlation across the sample was established at a well-defined sample thickness-dependent temperature $T_{\text{th}}(d, H)$. At $T_{\text{th}}(d, H)$, the resistivity in the c direction $\rho_c(H, T)$ drops abruptly, and the resistivity in the ab plane $\rho_{ab}(H, T)$ of phase-correlated vortices across the sample decreases [6] and becomes zero at a thickness-independent temperature $T_i(H)$, where the vortex liquid-solid transition takes place. In BSCCO, no vortex phase correlation [7] across the sample in the c direction was established in the liquid region of the H-T phase diagram. From these transport properties of the two paramount high T_c superconductors, we expect that, if the maximum of the Nernst signal is due to the decrease of vortex mobility, it should take place at the proximity of $T_{\text{th}}(d, H)$ in YBCO and of $T_i(H)$ in BSCCO.

To study the relevance of the vortex phase correlation in the field direction, we measured $e_N(T, H)$ and the resistivity of optimally doped single crystals of YBCO and BSCCO with and without columnar defects (CDs) for the $\mathbf{B} \parallel \mathbf{c}$ axis. In twinned YBCO crystals, the sample thickness-dependent flux cutting and reconnection induce the field- and temperature-dependent maximum of $e_N(T, H)$ but do not contribute to the vortex transport entropy. We show that the maximum in $e_N(T, H)$ in YBCO below T_c is induced by the size-dependent vortex

mobility. While in YBCO the vortices in the liquid state are accepted to respond as a three-dimensional system, in BSCCO the vortices are considered to be [8] uncoupled pancakes nucleated on Cu-O planes. We have found that the maximum in the Nernst voltage below T_c in BSCCO is not associated with the vortex mobility in the liquid state but to an intrinsic change of the temperature dependence of S_ϕ of vortices in this phase.

The YBCO and BSCCO single crystals were grown as described in Refs. [6,9]. The columnar defects, nearly parallel to the c axis, with a dose equivalent field of $B_\phi = 3$ T were created by irradiation with 278 MeV Sb^{24+} for BSCCO and 309 MeV Au^{26+} ions for YBCO at TANDAR irradiation facility, Argentina. The ion tracks are of the order of the coherence length of both materials (5–10 nm in diameter). The T_c's of the nonirradiated samples used in the Nernst and the electrical resistance experiment were $T_c = 91.0$ and 91.3 K, respectively, for BSCCO and 93.6 K for YBCO. The irradiated samples have $T_c = 90.2$ K for BSCCO and $T_c = 91.7$ K for YBCO. The samples thickness were 20–40 μm for the nonirradiated samples and 8–15 μm for the irradiated ones. The Nernst [10] and the electrical resistance [6] measurement setups were described elsewhere.

In Fig. 1(b), we show $e_N(T, H)$ and the electrical resistivity of YBCO crystals for $H = 5$, 6, and 8 T with and without CDs. Once the vortex system melts, the mobility is finite, and $e_N(T, H)$ grows fast with a temperature up to a maximum at $T_{\max}(H)$. At higher temperatures, the Nernst voltage decreases towards the almost zero normal state value at temperatures well above T_c. The mobility edge of the irradiated sample moves to higher T and so does the corresponding $T_{\max}(H)$. The data suggest that $e_N(T, H)$ between the mobility edge and $T_{\max}(H)$ is strongly determined by pinning.

More importantly, $e_N(T, H)$ of samples with and without CDs coincides, within experimental uncertainty, at temperatures equal and above $T_{\rm id}(H)$ as shown by a tilted arrow in Fig. 1(b). It is found that the resistivities of the samples with and without CDs become equal in the same range of temperatures; see Fig. 1(b). This is observed in the whole range of field investigated, from 2 to 10 T, suggesting that for $T \geq T_{\rm id}(H)$ the columnar defects and, possibly, all other types of pinning centers, are irrelevant for the vortex response to a gradient of temperatures or electrical currents. Thus, ρ_{ab}, e_N, and consequently the entropy of samples with and without CDs coincide for $T \geq T_{\rm id}(H)$.

From the previous discussion and experimental observation, we define $T_{\rm id}(H)$ as the highest temperature where vortex pinning is effective, as determined by e_N measurements. Above $T_{\rm id}(H)$, the pinning potential becomes irrelevant, independently of the type or strength of the pinning potential. As we demonstrate below for $T < T_{\rm id}(H)$, not only the pinning potential of the columnar defects is switched on but also that associated with the defects in the nonirradiated sample as made evident by the behavior

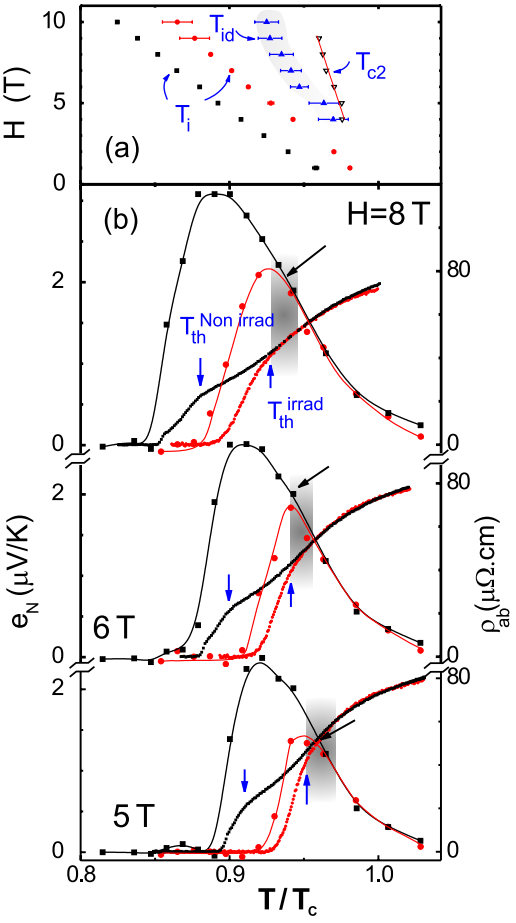

FIG. 1 (color online). (a) H-T diagram. The lines $T_{\rm id}$ (up triangles) and T_{c2} (down triangles and linear fit) and the irreversibility lines T_i for the irradiated (circles) and nonirradiated samples (squares) are shown. (b) Nernst signal e_N and electrical resistivity ρ_{ab} vs T/T_c in YBCO at $H = 5$, 6, and 8 T for the irradiated (circles) and nonirradiated samples (squares). $T_{\rm th}$ of both samples are indicated with arrows following Refs. [6,16]. Gray regions in both panels are equivalent.

of $\rho_{ab}(H, T)$ [see Fig. 1(b)] and the corresponding transport entropy of the vortices. This makes $T_{\rm id}(H)$ a relevant line in the phase diagram of the liquid state of vortex lines. The gray region in Fig. 1(b) indicates the experimental uncertainty for $T_{\rm id}(H)$. In Fig. 1(a), the line $T_{\rm id}(H)$ is plotted together with the pinning potential-dependent solid-liquid phase transition lines $T_i(H)$.

From the definition of $T_{\rm id}(H)$ we recognize that, for $T \geq T_{\rm id}(H)$, $U_\phi(T, H) = TS_\phi(H, T)$ should be the same for the YBCO samples investigated, independently of the type of pinning potential characterizing the transport properties at lower temperatures. Therefore, $U_\phi(T, H)$ becomes an intrinsic property of the ideal vortex system for $T \geq T_{\rm id}(H)$.

In Fig. 2, we plot $U_\phi(T, H)$ of samples with and without CDs as a function of temperature at 8 T. The data are representative of $U_\phi(T, H)$ in the whole range of fields investigated. We see that both $U_\phi(T, H)$ coincide not only for $T \geq T_{\rm id}(H)$ but also in a broader range of temperatures

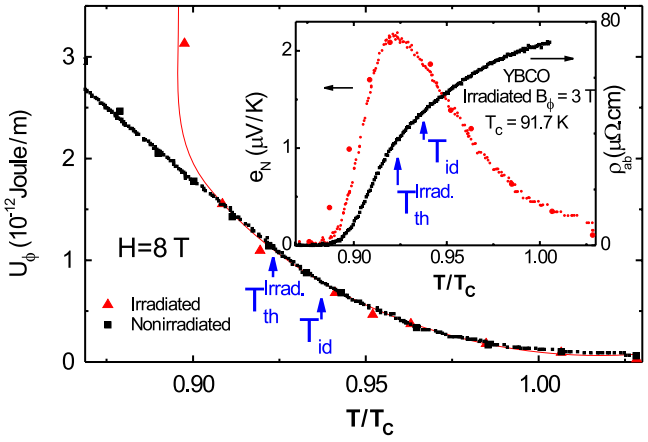

FIG. 2 (color online). U_ϕ vs T/T_c in YBCO at $H = 8$ T for the irradiated (red triangles plus line) and the nonirradiated sample (black squares, interpolation with small symbols). Inset: Measured e_N and ρ_{ab} (red circles and black squares, respectively) and recalculated e_N (small red circles) for the irradiated crystal.

below $T_{id}(H)$. This demonstrates that the maximum of $e_N(H, T)$ is induced only by the effective pinning potential acting on electrical transport properties; see the inset in Fig. 2 for the results in the irradiated sample. Somewhat below its $T_{th}(H)$, $U_\phi(T, H)$ shows an anomalous increase when decreasing temperature as compared to that of the nonirradiated sample. The analysis of this feature helped to understand the relative contribution of ρ_{ab} and S_ϕ to e_N in YBCO.

We see from Fig. 2 that $U_\phi(T, H)$ of the nonirradiated sample increases linearly when decreasing T well below the $T_{th}(H)$ of the irradiated sample. This linear dependence is expected in a mean field description [1], and its extrapolation to $U_\phi(T, H) = 0$ provides a mean field $T_{c2}(H)$, also plotted in Fig. 1(a). The results support the idea that the measured $U_\phi(T, H)$ is that of an intrinsic bulk superconductor, independently of the amount and type of pinning centers. Assuming this, we calculated the $e_N(H, T)$ of the sample with CDs using its measured ρ_{ab} and the $U_\phi(H, T)$ from the sample without CDs, as plotted in the inset in Fig. 2. The results are important and revealing. We see that the calculated $e_N(H, T)$ reproduces the experimental data within the experimental error from temperatures well above T_c to somewhat below the temperature at the maximum. More importantly, the calculated data extrapolate to the same $T_i(H)$, detected by electrical transport. This result makes evident the origin of the anomalous raise of $U_\phi(T, H)$ at temperatures below the maximum, in both samples. The thermal gradient used to determine the Nernst effect induces a force that exceeds the extremely small linear response regime close to the solid-liquid transition [11]. The thermal force in this range of temperatures is calculated to be [12] up to 1 order of magnitude larger than that used in electrical measurements. The results show that the maximum of $e_N(H, T)$ in YBCO is a size effect that reflects the growth of the vortex phase coherence in the c direction. The maximum takes place close to $T_{th}(d, H)$ where the c axis vortex phase correlation length coincides with the sample thickness.

While the maximum occurs at a thickness-dependent temperature, the inflection of the Nernst signal occurs at the thickness-independent $T_{id}(H)$. A remarkable result associated with $T_{id}(H)$ is that in this line the linear temperature dependence characteristic of a mean field behavior of U_ϕ is lost; see Fig. 2. At higher temperatures, the curvature of $U_\phi(T, H)$ indicates the dominant contribution of thermal fluctuations, insensitive to the presence of structural defects. In this sense, $T_{id}(H)$ might well be an experimental verification of that proposed by Nguyen and Sudbø [13], where thermally induced vortex loop proliferation causes the loss of vortex line tension.

The Nernst signal and electrical resistivity of BSCCO samples with and without CDs for fields from 1 to 16 T were measured. Figure 3(a) shows typical results, in this case for 3 and 5 T. In BSCCO, we found that the absolute

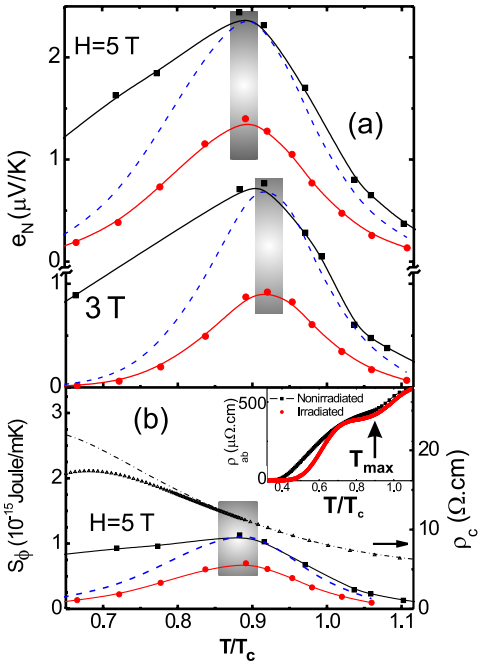

FIG. 3 (color online). (a) Nernst signal e_N at $H = 3$ and 5 T vs T/T_c in BSCCO. Red circles and black squares curves correspond to the irradiated ($B_\phi = 3$ T) and nonirradiated sample, respectively. The dashed curves correspond to the Nernst signal of the irradiated sample normalized at the corresponding maximum of the nonirradiated one. The shading emphasizes the maximum region. (b) Entropy per unit vortex length S_ϕ ($S_\phi = e_N\phi_0/\rho_{ab}$) vs T/T_c in BSCCO at $H = 5$ T for the irradiated (red circles) and the nonirradiated samples (black squares). The dashed curve corresponds to S_ϕ of the irradiated sample normalized at the corresponding maximum of the nonirradiated one. The ρ_c vs T/T_c at $H = 5$ (up triangles) and 8 T (dashed-dotted line). The inset shows ρ_{ab} at $H = 5$ T for the samples with (red circles) and without CDs (black squares).

value of $e_N(H, T)$ of the sample with CDs is systematically smaller than that of the nonirradiated sample. It is remarkable that for $T \geq T_{\max}(H) = T_{\mathrm{id}}(H)$ the ratio of $e_N(H, T)$ between the irradiated and nonirradiated samples is only a function of H and not of temperature [14]; see Fig. 3(a).

At first glance, some similarities are found between the results of BSCCO and YBCO: For $T \geq T_{\mathrm{id}}(H)$, the $e_N(H, T)$ of YBCO as well as the normalized $e_N(H, T)$ of BSCCO in samples with and without CDs coincide up to temperatures well above their respective T_c; for $T \leq T_{\max}(H)$, $e_N(H, T)$ goes to zero at the corresponding $T_i(H)$ in each material. On the other hand, differences are evident. Contrary to what is measured in YBCO, $T_{\max}(H)$ of BSCCO is the same for samples with and without CDs, as well as for samples of different thicknesses [2]; in YBCO, the rapid decrease of $\rho_{ab}(H, T)$ in each type of sample determines the maximum of $e_N(H, T)$; in BSCCO, $\rho_{ab}(H, T)$ is independent of the presence of CDs to temperatures well below $T_{\max}(H)$; see the inset in Fig. 3(b). The analysis of $e_N(T, H)$ and $\rho_{ab}(H, T)$ for samples with and without CDs allows the detection of magnitudes associated with the equilibrium thermodynamic state of the vortex system. In YBCO, $T_{\max}(H)$ is determined by the behavior of $\rho_{ab}(H, T)$ approaching $T_i(H)$. Thus, the maximum of $e_N(H, T)$ is not associated with an equilibrium state. On the contrary, that maximum in BSCCO is determined by the maximum of an equilibrium property $S_\phi(H, T)$ [Fig. 3(b)] for all fields and temperatures studied [12]. This is an interesting and puzzling result: While the vortex mobility $\rho_{ab}(H, T)$ as well as the temperature $T_{\max}(H) = T_{\mathrm{id}}(H)$ remain unaffected by the nature of the pinning potential for temperatures in the neighborhood of the maximum of $e_N(H, T)$, it is the thermodynamic equilibrium property $S_\phi(H, T)$ that becomes dependent on the type of structural defects for $T < T_{\mathrm{id}}(H)$. The liquid vortex state in BSCCO is accepted to be [8] that of 2D uncoupled vortices nucleated in Cu-O planes. On the other hand, the data in this work show that below the temperature $T_{\mathrm{id}}(H)$ (identical for samples with and without CDs) $S_\phi(H, T)$ becomes dependent on the type of structural defects. Thus, the order induced by correlated defects below $T_{\mathrm{id}}(H)$ requires a change of the nature of the vortex system at this temperature. This is supported by the incipient decrease of $\rho_c(T, H)$ from the nonmetallic normal state at $T_{\mathrm{id}}(H)$ in both samples; see Fig. 3(b). This points out that for $T < T_{\mathrm{id}}(H)$ the interaction between pancakes vortices in the neighbor Cu-O planes should not be disregarded. This interaction could induce a change of the effective dimensionality of the vortex system in BSCCO, decreasing the configurational entropy contribution [15] in the presence of columnar defects.

In conclusion, transport and Nernst measurements in samples with and without correlated defects reveal the origin of the maximum of the Nernst signal in the liquid state of dissimilar vortices. In YBCO, vortex cutting and reconnection [5] induce a sample size-dependent $T_{\max}(H)$, well below the corresponding $T_{\mathrm{id}}(H)$. In this case, the vortex transport entropy remains independent of the nature of defects. On the contrary, in BSCCO, the maximum is due to the intrinsic maximum of the vortex transport entropy, suggesting a change of the effective vortex dimensionality below the well-defined temperature where the resistance in the c direction starts to deviate from its normal state value.

We acknowledge correspondence with L. Bulaevskii and D. Huse. We thank L. Civale and H. Lanza for the irradiation and E. E. Kaul and N. Saenger for help with sample preparation and measurements. G. B. and G. N. acknowledge financial support from CONICET-Argentina.

*bridoux@cabbat1.cnea.gov.ar

[1] A. M. Campbell and J. E. Evetts, Adv. Phys. **50**, 1249 (2001), and references therein.
[2] H.-C. Ri, R. Gross, F. Gollnik, A. Beck, R. P. Huebener, P. Wagner, and H. Adrian, Phys. Rev. B **50**, 3312 (1994).
[3] Y. Wang, L. Li, and N. P. Ong, Phys. Rev. B **73**, 024510 (2006), and references therein.
[4] D. S. Fisher, Phys. Rev. B **31**, 1396 (1985); F. de la Cruz, J. Luzuriaga, E. N. Martinez, and E. J. Osquiguil, Phys. Rev. B **36**, 6850 (1987).
[5] G. Blatter, M. V. Feigel'man, V. B. Geshkenbein, A. I. Larkin, and V. M. Vinokur, Rev. Mod. Phys. **66**, 1125 (1994).
[6] F. de la Cruz, D. López, and G. Nieva, Philos. Mag. B **70**, 773 (1994).
[7] H. Safar, E. Rodriguez, F. de la Cruz, P. L. Gammel, L. F. Schneemeyer, and D. J. Bishop, Phys. Rev. B **46**, 14 238 (1992); R. Busch, G. Ries, H. Werthner, G. Kreiselmeyer, and G. Saemann-Ischenko, Phys. Rev. Lett. **69**, 522 (1992).
[8] L. N. Bulaevskii, A. E. Koshelev, V. M. Vinokur, and M. P. Maley, Phys. Rev. B **61**, R3819 (2000).
[9] E. E. Kaul and G. Nieva, Physica (Amsterdam) **341C–348C**, 1343 (2000).
[10] G. Bridoux, P. Pedrazzini, F. de la Cruz, and G. Nieva, Physica (Amsterdam) **460C–462C**, 841 (2007).
[11] S. A. Grigera, E. Morré, E. Osquiguil, C. Balseiro, G. Nieva, and F. de la Cruz, Phys. Rev. Lett. **81**, 2348 (1998).
[12] G. Bridoux, Ph.D. thesis, Instituto Balseiro, 2008 (unpublished).
[13] A. K. Nguyen and A. Sudbø, Phys. Rev. B **60**, 15 307 (1999).
[14] The ratio of the absolute values of S_ϕ for samples without and with CDs above $T_{\max}(H)$ in BSCCO varies as $B_\phi/H + 1$.
[15] S. Mukerjee and D. A. Huse, Phys. Rev. B **70**, 014506 (2004).
[16] E. F. Righi, S. A. Grigera, D. López, G. Nieva, F. de la Cruz, L. Civale, G. Pasquini, and P. Levy, Phys. Rev. B **55**, 5663 (1997).